

Adaptive fault ride through control of VSM Grid-Forming Converters

T. Lin, M. K. Das, A. M. Gole, A. Isaacs

Abstract—Recently, many high voltage direct current (HVdc) transmission lines are being constructed with the intention of becoming “backbones” of future power grids. Grid-Forming (GFM) controlled Voltage Source Converters (VSCs) are anticipated to provide significant stability advantages compared with Grid-Following (GFL) VSCs in HVdc converters connected to weak ac grids or to grids with high penetration of renewable inverter-based resources (IBRs). This paper proposes an adaptive fault ride through controller for Virtual Synchronous Machine (VSM) GFM control, which has significantly improved fault ride through capability over the more conventional GFM with cascaded or switchable current limiting. The performance of the proposed adaptive control is investigated using Electromagnetic Transient (EMT) simulation. The results show that the proposed adaptive control has superior post disturbance recovery from ac faults as well as phase angle shifts, and overcomes the instability reported in GFMs connected to strong ac networks.

Keywords: VSC-HVdc, Grid-Forming (GFM) control, Virtual Synchronous Machine (VSM), fault-ride through, phase angle jump ride through.

I. INTRODUCTION

Increasing levels of inverter-based resources (IBRs) in the power system are posing new challenges to power system stability. Most power electronics converters currently in service are of the “Grid Following” (GFL) type [1], [2], and rely on fast synchronization with the external grid. A phase-locked loop (PLL) is used to rapidly track the phase of the grid ac voltage and the converter switches are operated to produce a voltage of desired magnitude and phase offset relative to the tracked phase angle.

However, GFL converters find it difficult to remain synchronized when the PCC voltage can change rapidly in magnitude and phase, as in the case when connected to weak ac grids. For VSC-HVdc systems, the Phase-locked loop (PLL) gain greatly affects the operation, particularly in a weak grid condition [3]. Moreover, unlike synchronous generators, GFL converters do not provide significant short circuit capacity and self-synchronization capability.

In contrast, a Grid-forming (GFM) converter [4], [5], is not designed to tightly synchronize with an external reference voltage, but rather to generate its own terminal voltage which is held relatively constant within the transient time frame and sometimes longer. VSC islanded control is an early version of GFM [6] control. It is used when the VSC-HVdc converters are connected to a weak ac system or for black starting the ac system [7]. However, islanded control is primarily intended for applications with passive ac loads or limited generation and shows its limitations when the synchronous generation in the ac

system becomes comparatively large [8].

A virtual synchronous machine (VSM) type GFM control [9], [10] imparts the characteristic of a synchronous generator which allows the converters to provide stability in the controls and maintain synchronism with the external grid during in weaker grids. Various VSM control methods have been proposed to emulate the behavior of the real synchronous machine with different levels of accuracy. Some use a simple voltage source representation that emulates the electromechanical swing equation [19][20]. Others emulate a synchronous machine in more detail, but reference [18] shows that this can introduce synchronous resonance and can also be more challenging to tune in comparison with the swing equation-based implementations. Another popular GFM technique is droop-based GFM control [11], [12], where the system frequency order is made proportional to the active power. References [13], [14] demonstrate the equivalence between Droop-based GFM and a swing equation based VSM GFM control.

GFM converters are typically equipped with a current limiter to prevent overcurrent damage to the power electronics. Reference [23] has shown that if the limit is encountered, the GFM can show poor fault recovery and even become unstable in strong ac networks. To address this, adaptive virtual impedance control [21][22] has been proposed for the GFM to limit fault current and damp the post fault oscillation. This paper proposed an adaptive fault ride through control, which embodies dynamically changing the control parameters in the power synchronization loop of the GFM that improves its post fault recovery for both weak and strong systems.

IEEE Standard 2800-2022 [24] states that any VSC should be able to ride through a phase change in ac voltage of +/- 25 degrees. Such a phase change can occur due to ac power flow change resulting from connecting or disconnecting a transmission line. One contribution of this paper is that it demonstrates that due to the GFM’s inertia response, a sudden jump in the system phase angle can result in the GFM converter losing synchronism. It also shows that this problem can be mitigated with the proposed adaptive controller.

The paper first shows an example of poor recovery from a solid ac fault in a VSM GFM using typical configurations in previous literature [15], [16], [17]. The proposed adaptive control approach transiently changes the active power order and damping coefficient in its power synchronization loop. Using EMT simulation, this approach is shown to significantly improve its post fault recovery in comparison to traditional GFM control.

The superior performance of the VSM GFM equipped with adaptive controller for stably riding through phase angle jumps is also demonstrated by comparing its response with that of a conventional VSM.

II. VIRTUAL SYNCHRONOUS MACHINE GRID-FORMING CONTROL

In this section, the control strategies of the VSM GFM with current limiting are explained.

In VSM-GFM, the MMC is made to mimic a real synchronous machine, using various different levels of fidelity, which can vary from simplified swing equation dynamics to detailed electromechanical models including amortisseur windings, exciters and governors. This paper uses a swing equation based simplified synchronous machine emulation for the VSM. Although higher order models that include a more detailed machine representation are possible [25][26], reference [18] have shown that they do not offer a significant performance improvement.

Fig. 1 shows the GFM control structure with a cascaded current controller. The power synchronization loop above the dotted line emulates the swing equation of a synchronous machine. J is the virtual inertia constant and D is the damping coefficient. Like a synchronous machine, the power synchronization control of a VSM uses the swing equation to generate the ac voltage synchronization angle θ at the Point of Common Coupling (PCC). An ac voltage control loop is included for regulating ac voltage. The q-axis voltage reference V_{qref} of the ac voltage control loop is set to zero, while the d-axis voltage reference V_{dref} is set to the grid voltage reference V_{ac_ref} . In order to limit overcurrent, an inner decoupled current control loop [15][17] is present. The voltage control loop generates the necessary d and q axis current references i_{dref} and i_{qref} . Overcurrent is limited by adding limits to i_{dref} and i_{qref} . Different limiting approaches are possible, such circular limiting, where the magnitude $\sqrt{i_d^2 + i_q^2}$ of the ac current is limited, but the phase angle $\tan^{-1}(i_d/i_q)$ retained. Alternatively, i_d or i_q priority control is often employed. In this paper the controller uses i_d priority which is often used in HVdc systems for better recovery from ac faults [27].

The necessary voltage orders V_{cd} , V_{cq} are generated to achieve the ordered currents, from which the required output voltage order V_{ac_ref} is computed. The inner current control loop imparts effective control of current and is always in-line for normal as well as faulted operation to limit the current.

Alternatively, it is also possible to have a switchable current control [16], where the main mode of control is voltage control, and a separate current control is switched in only when overcurrent occurs shown in Fig. 2.

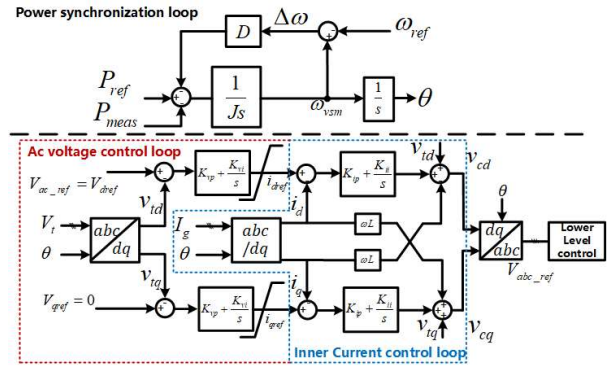


Fig. 1. control structure of a GFM VSC with cascaded current limiting

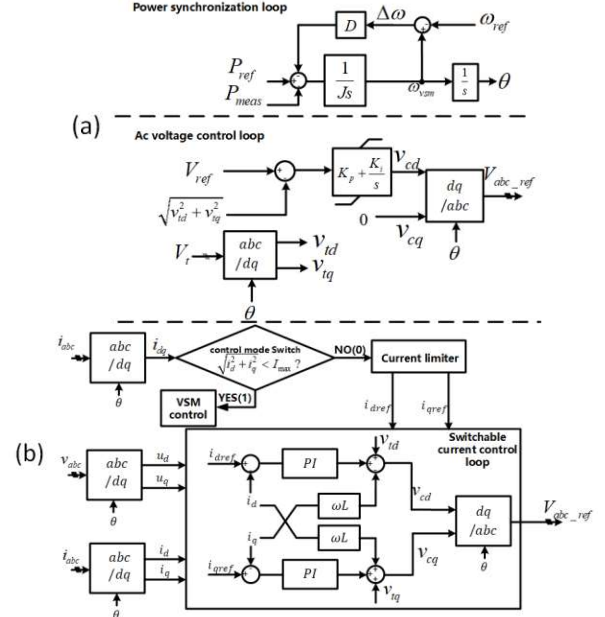


Fig. 2. control structure of a GFM VSC with switchable current limiting (a) normal operation (b) current limiting mode

III. PROBLEMS WITH VSM GFM POST FAULT RECOVERY AND IMPROVEMENTS THROUGH PROPOSED ADAPTIVE CONTROL

This section demonstrates the poor fault recovery in VSM GFM connected to strong ac networks and in order to mitigate it, proposes a new adaptive control strategy in which the VSM's parameters are dynamically changed during the disturbance event. A test system with a VSM GFM connected to an ac system is modelled in an EMT simulation program (PSCAD/EMTDC) to study the fault ride through performance. The VSM GFM is implemented using an MMC and the current limiting can be selected to be either of the in-line cascaded or switchable type. The connected ac system is represented by a Thevenin equivalent voltage source behind an impedance as shown in Fig. 3. Its parameters are adjustable to provide the SCR under study.

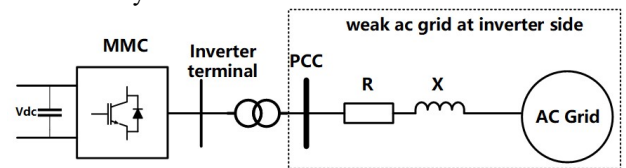


Fig. 3. Test scenario of the MMC connected to a Thevenin equivalent voltage source behind impedance.

The MMC parameters are given in TABLE I. The remote converter of the MMC-HVdc system is assumed to be in dc voltage control, and so is represented as a +/- 250 kV constant dc voltage.

TABLE I
MMC-HVDC SPECIFICATIONS

MMC-HVdc pole configuration	symmetrical monopole
DC link voltage	+/- 250 kV
Rated power	1000 MVA
Submodule number in each arm	200
Converter transformer winding voltage	230 kV/250 kV
Converter transformer leakage reactance	0.18 pu
Arm inductor	24 mH
Submodule capacitance	10.6 mF
Rated ac system voltage	230 kV, 60 Hz

A. Post Fault recovery of VSM GFM

An EMT simulation is conducted to test the fault ride through performance of the VSM GFM depicted in Fig. 1 with weak and strong ac networks. First, the weak system case is simulated, with the VSM GFM connected to an ac system of SCR=1.0. Control parameters are shown in TABLE II below.

TABLE II
VSM GFM WITH CASCADED CURRENT CONTROL KEY CONTROL PARAMETERS

Inertia constant J	0.5 s
Damping coefficient D	20 pu
Active power order P_{ref}	1 pu
Ac voltage reference $V_{ac,ref}$	1 pu
Ac voltage controller (K_{vp} , K_{vi})	(7, 10)
Inner current controller (K_{ip} , K_{ii})	(0.5, 100)

A solid three-phase to ground fault is applied at PCC bus of the test system shown in Fig. 3 at $t = 5$ s. The fault duration is 0.2 s and the maximum current limit is set to 1.3 pu. Plots of the rms ac current, rms terminal voltage and output power are shown in Fig. 4 (a), (b) and (c) respectively. Although the current limiting control loop works well limiting the fault current to the given limit of 1.3 pu, there is an overvoltage of 1.4 pu and transient reversal of power (up to -1 pu) during post fault recovery period.

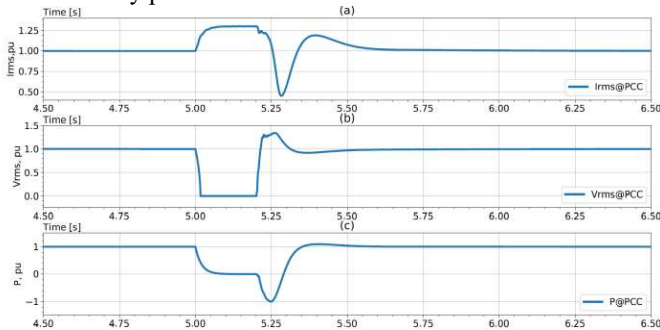


Fig. 4. VSM GFM with cascaded current control (a) ac current output (b) ac voltage at PCC and (c) active power output. (SCR=1)

Fig. 5 (a) and (b) show the phase angle θ of the VSM's

voltage output and its angular frequency ω_{vsm} as in Fig. 1. The transient power reversal can be attributed to the large variation of the ac voltage phase angle (0° to -140°) of the VSM GFM. As shown later in Fig. 6, for a strong ac network, this could lead to loss of synchronism.

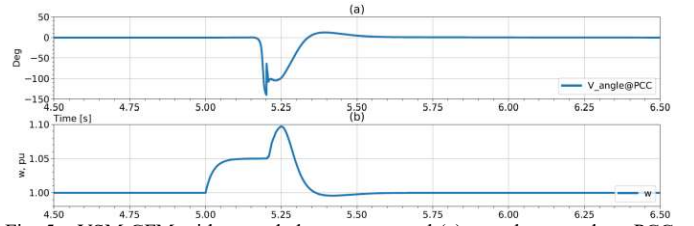


Fig. 5. VSM GFM with cascaded current control (a) ac voltage angle at PCC and (b) synchronous speed ω_{vsm} measured from GFM power synchronization loop. (SCR=1)

Now we investigate what happens when the connected ac system becomes stronger. The performance of VSM GFM with connected ac systems ranging from weak (SCR =1) to very strong (SCR=10) are shown in Fig. 6. In Fig. 6, (a) is the ac current output from the converter, (b) is the ac voltage at PCC, and (c) is the active power output from the converter. Note for a strong ac system, e.g., SCR = 10, the system fails to ride through the ac fault. Previous literature has reported this phenomenon, but without giving any reason. We attribute this being due to the small ac side impedance in the strong ac system, which can precipitate a very large power and overcurrent transient even for a small phase angle difference between VSM and the ac system (represented by an ac voltage source). This can be observed from the active power plot in Fig. 6 (c), where the loss of synchronism is obvious.

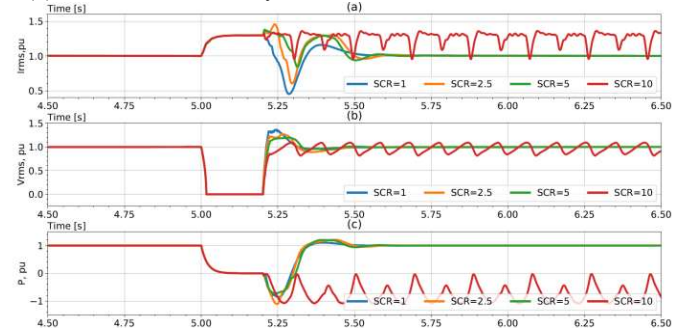


Fig. 6 VSM GFM with Cascaded current control (a) ac current output (b) ac voltage (c) active power output

Again, the post-disturbance transient reversal of power direction is noticeable in Fig. 7 (c). The same qualitative conclusion can be drawn if current limiting is achieved by switchable current limiting control as in Fig. 2, with key control parameters as shown in TABLE III. Results are shown in Fig. 7, which plots (a) ac current output from the converter, (b) ac voltage at PCC, (c) active power output from the converter, and (d) current control loop (CCL) switch signal (CCL=0 meaning current control is not active, CCL=1 means current control is activated.) Again, for the strong ac network, (e.g., SCR=5 or 10), a loss of synchronism is clearly observed.

TABLE III
VSM GFM WITH SWITCHABLE CURRENT CONTROL KEY CONTROL
PARAMETERS

Inertia constant J	0.5s
Damping coefficient D	20 pu
Active power order P_{ref}	1 pu
Ac voltage reference V_{ac_ref}	1 pu
Ac voltage controller (K_{vp} , K_{vi})	(0.1, 5)
transient current controller (K_{ip} , K_{ii})	(0.5, 100)

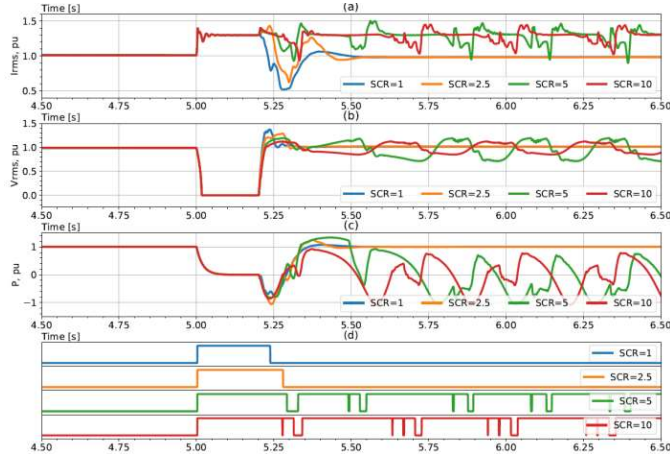


Fig. 7 VSM GFM with Switchable current control (a) ac current output (b) ac voltage at PCC (c) active power output and (d) current control loop switch signal

B. Adaptive Fault Ride Through Control on VSM GFM

The undesirable transient reverse power and overvoltage discussed above can be avoided by limiting the voltage angle change to a small range, which can be achieved by limiting the change of the synchronous speed ω_{vsm} from the GFM power synchronization loop in Fig. 1 during fault.

During a solid three-phase to ground fault, the active power output from the GFM converter is close to 0. According to the swing equation, the synchronous speed will increase until $d\omega/dt = 0$, as shown in the following equation:

$$P_{ref} - D\Delta\omega = J \frac{d\omega}{dt} = 0 \quad (1)$$

Thus, decreasing the active power order P_{ref} and increasing the damping coefficient D in the VSM can decrease the synchronous speed change $\Delta\omega$ during the fault. If $\Delta\omega$ is small, the voltage angle change can be limited to a small range during the current limiting period. Then the large resynchronization transient of the VSM GFM converter during the post fault period can be avoided.

It should be noted that the virtual synchronous machine gives more flexibility than a real machine, because the VSM's parameters can be changed at will and even dynamically. Thus, in this paper, an adaptive fault ride through control mode shown in Fig. 8 is proposed targeting on cancelling the post fault transient. When an overcurrent is sensed by the VSM, its power order P_{ref} is transiently decreased, and its damping coefficient D is transiently increased. When the overcurrent

diminishes, P_{ref} and D are returned to their normal setting values.

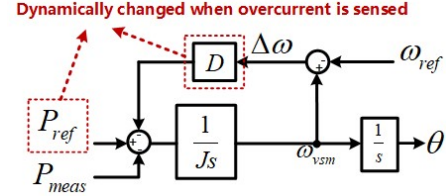


Fig. 8 Proposed adaptive fault ride through control mode.

The proposed adaptive change method is tested on a VSM with cascade current control in the MMC test system shown in Fig. 3. The active power order P_{ref} and damping coefficient D transiently changes from 1 pu to 0.5 pu and from 20 pu to 220 pu respectively when the ac current is over 1.3 pu. Fig. 9 compares the voltage angle and the synchronous speed for the case with adaptive control (orange) and without adaptive control (blue). Instead of a phase angle change in the range of $[0, -140]$ degrees, the phase change is much improved and confined to a smaller interval of $[20, -20]$ degrees.

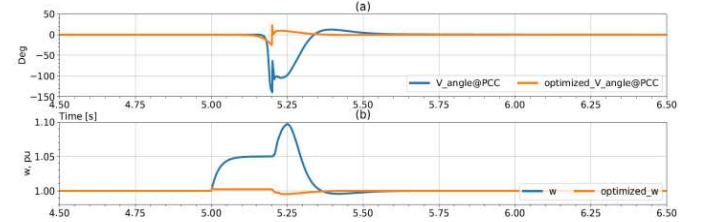


Fig. 9 Improved (a) ac voltage angle at PCC and (b) synchronous speed ω_{vsm} measured from GFM power synchronization loop, with proposed adaptive control method. (VSM with cascaded current control)

Fig. 10 shows the EMT simulation results of (a) ac current output from the converter, (b) ac voltage at the PCC bus, (c) active power output and (d) adaptive control switched on signal for SCRs ranging from 1 to 10. It is evident that the ac voltage and active power recovery are much smoother with the adaptive fault ride through control.

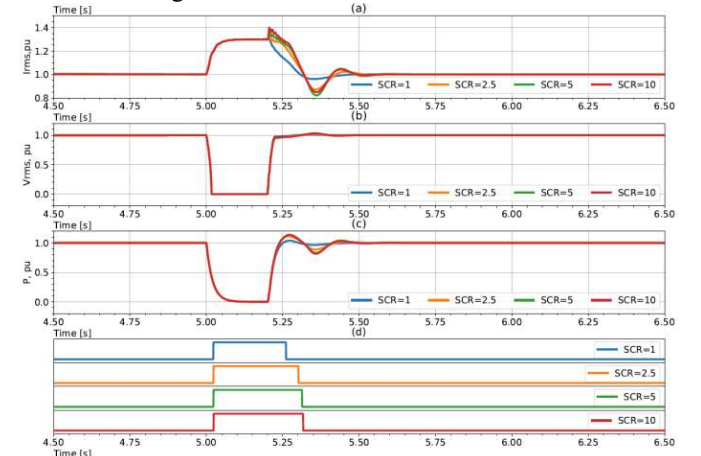


Fig. 10. Adaptive fault ride through control on VSM GFM with Cascaded current control (a) ac current output (b) ac voltage at PCC (c) active power output and (d) adaptive control switched on signal.

If adaptive fault ride through control is implemented with switchable current limiting of Fig. 2, a similar improvement also accrues. The adaptive fault ride through control is activated

when the current control loop is switched in. Fig. 11 shows the results for SCRs ranging from 1 to 10, when the adaptive fault ride through control is used. Compared with the conventional switchable current limiting results shown in Fig. 7, the proposed adaptive control method greatly improves the fault ride through performance of VSM GFM with switchable current control connected to both weak and strong systems.

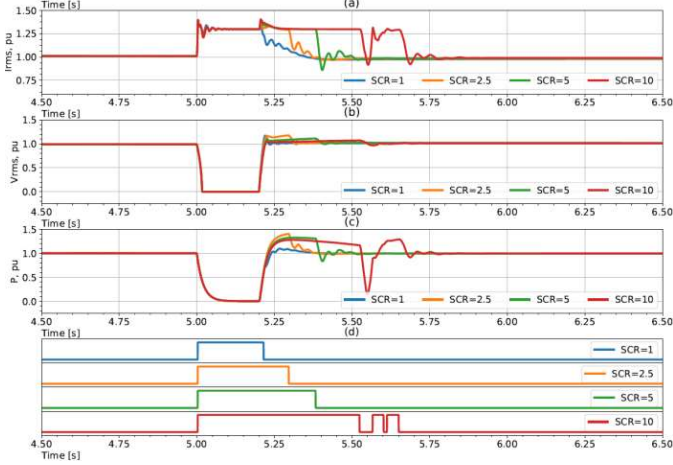


Fig. 11 Adaptive fault ride through control on VSM GFM with Switchable current control (a) ac current output (b) ac voltage at PCC (c) active power output and (d) current control loop switch signal

IV. IMPROVEMENT OF VSM GFM PHASE ANGLE JUMP RIDE THROUGH WITH PROPOSED ADAPTIVE CONTROL

A. VSM GFM response on ac system phase angle jump

We will show that for sudden phase changes in grid voltage as can be precipitated by power flow change due to line switching, the traditional VSM GFM even has worse performance than the Grid Following Converter (GFL), but this can be rectified with the use of the proposed adaptive control strategy. IEEE Standard 2800-2022 [24] demands that any VSC should be able to ride through a phase change in ac voltage of +/- 25 degrees.

Consider the same test system of Fig. 3 used in the previous sections with $SCR = 2.5$. The GFL control key parameters used in the following test are shown below in TABLE IV.

TABLE IV
GFL CONTROL KEY PARAMETERS

Normal operation PLL gain (K_p, K_i)	(50, 900)
Ac voltage controller (K_{vp}, K_{vi})	(0.5, 10)
Inner current controller (K_{ip}, K_{ii})	(0.5, 100)

A phase angle shift is applied to the Thevenin equivalent voltage source to emulate the ac voltage phase angle change close to the PCC bus, which could be precipitated by some grid events e.g., power flow change. The phase of the ac source is reduced by 30 degrees at 5 s, and then increased back to 0 degree at 7 s.

First consider the case without the proposed adaptive control and the current limiter set to a very high value, so that current limiting does not occur in the example. The ac system has an $SCR=2.5$. Consider the VSM GFM with the control structure

shown in Fig. 2 (a). The inertia constant is $J=5$ s. Fig. 12 shows (a) voltage angle at PCC, (b) ac current output and (c) active power output of GFL (blue) and VSM GFM (orange) response to the connected ac voltage source phase jump. The VSM GFM converter responds to this phase angle change following the swing equation and the associated inertia inherent in the model, and hence gives a sluggish response. In contrast, the GFL synchronizes through a PLL (i.e., no inertia in the model) and shows a much faster response than the VSM GFM as seen in Fig. 12(a) blue and orange curves. The transient active power and ac current output change of the VSM GFM converter is larger than that of the GFL converter since the active power output is directly linked to the phase angle according to the swing equation, which can be observed in Fig. 12(b) and (c) blue and orange curves.

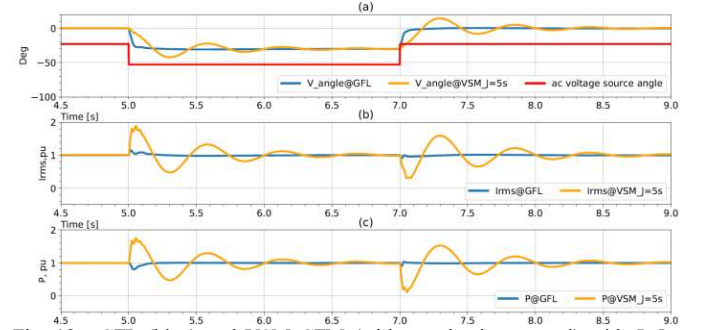


Fig. 12. GFL (blue) and VSM GFM (without adaptive control) with $J=5$ s (orange) response to a phase jump (30 degrees) (a) PCC voltage phase angle (b) ac current and (c) active power output.

So, for phase shift ride through, the GFL shows fast tracking behavior, but the VSM GFM has a sluggish response with more oscillation and a larger settling time. Next, we will show, that if current limiting is applied to 1.3 pu to the VSM GFM, the behavior deteriorates further and can even cause a failed recovery, as shown in the plots of Fig. 13. In the figure, (a) is the voltage phase angle at PCC, (b) the ac current output and (c) the active power output from the converter. During the phase angle jump, overcurrent occurs, and when the current limiting remains on for too long, the controller loses the ability to lock synchronization voltage angle θ , the VSM GFM can lose synchronization and the system becomes unstable. In this case, the VSM GFM inertia constant J is 5 s. The transient active power and ac current output change of VSM GFM is large and the current limiting is activated starting at $t = 5$ s. The voltage angle loses synchronism and becomes unstable due to the current limiting shown in Fig. 13 (a), (b) and (c).

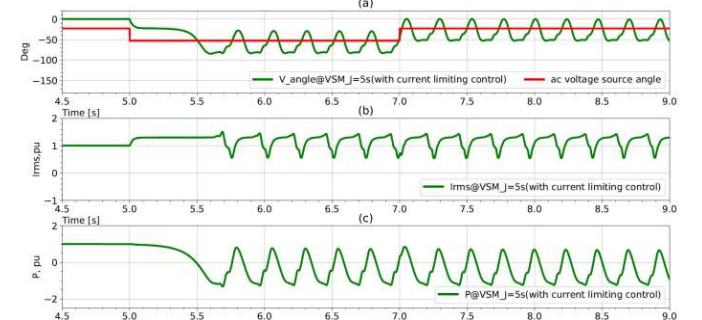


Fig. 13 (without adaptive control) VSM GFM ($J=5$ s) with current limiting

controls response to the connected ac voltage source phase jump. (a) ac voltage phase angle (b) ac current output and (c) active power output

B. Improved phase angle jump ride through performance on VSM GFM with Proposed Adaptive Control

Since the proposed adaptive fault ride through control can limit the synchronization voltage angle change during the overcurrent transient, it can also improve the VSM GFM phase angle ride through performance. The simulation results with the proposed adaptive control are shown in Fig. 14. The system is able to ride through the disturbance successfully, unlike the case without adaptive control in Fig. 13. The voltage angle is frozen when the adaptive control is switched on during the overcurrent limiting period. When the overcurrent limiting is over, the inertia behavior of the VSM GFM resumes, and thus not jeopardizing the GFM functionality during normal operation.

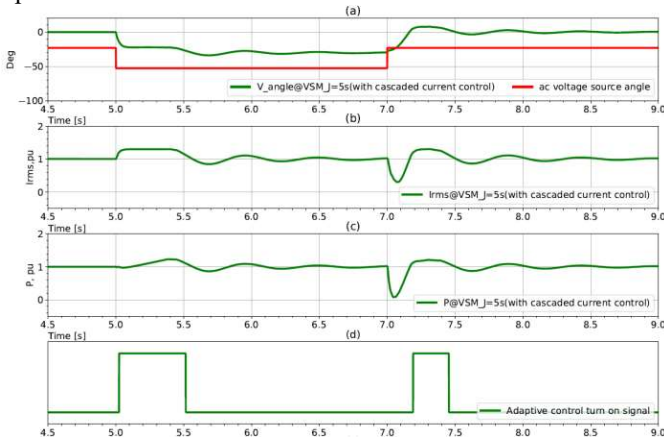


Fig. 14 VSM GFM ($J=5$ s) with cascaded current limiting and adaptive fault ride through controls response to the connected ac voltage source phase jump ($SCR=2.5$). (a) PCC voltage phase angle (b) ac current output (c) active power output and (d) adaptive fault ride through switched on signal

V. CONCLUSIONS

The paper proposes an adaptive fault ride through control mode for VSM GFM control to improve its post fault recovery transient and voltage phase angle jump ride through performance.

The EMT simulation shows the fault ride through performance of VSM GFM with cascaded or switchable current control can be optimized by transiently changing the active power order and the damping coefficient in its power synchronization loop. This greatly improves the VSM GFM converter post fault recovery, particularly when connected to strong ac systems, which was seen as a challenge for more classical GFM control methods. In addition to improved performance with strong ac systems, the performance with weak ac systems was also improved.

This paper identifies a problem with a GFM converter is that it can exhibit a slower response following a phase angle jump in comparison to a GFL converter. Nevertheless, the proposed adaptive fault ride through controller also improves the phase angle jump ride through performance and yet does not hamper its GFM functionality during normal operation.

VI. ACKNOWLEDGMENT

The authors gratefully acknowledge the contribution of D. A. Woodford, G. D. Irwin and other Electranix Corporation power system engineers for their suggestions on this paper.

VII. REFERENCES

- [1] J. Matevosyan, J. MacDowell, "A Future with Inverter-Based Resources". IEEE Power & energy, Volume 19, Number 6, pp.18-28, 2022.
- [2] Energy Systems Integration Group (ESIG) report, "Grid-Forming Technology in Energy Systems Integration", ESIG, 2022.
- [3] Zhou, J. Z., Ding, H., Fan, S., Zhang, Y., & Gole, A. M. (2014). "Impact of short circuit ratio and phase locked loop parameters on the small signal behavior of a VSC HVdc converter." IEEE Transactions on Power Delivery, 29(5), 2287–2296.
- [4] NERC Inverter-Based Resource Performance Working Group (IRPWG) report, "Grid Forming Technology: Bulk Power System Reliability Consideration". NERC, Dec. 2021.
- [5] J. Matevosyan, B. Badrzadeh, "Grid-Forming Inverters". IEEE Power & energy, Volume 17, Number 6, pp.89-98, 2019.
- [6] J. Rocabert, A. Luna, F. Blaabjerg, and P. Rodriguez, "Control of power converters in ac microgrids," IEEE Trans. Power Electron., vol. 27, no. 11, pp. 4734–4749, Nov. 2012.
- [7] "VSC transmission." Cigre Working Group B4.37-269, Tech. Rep., 2005.
- [8] "Guide for the Development of Models for HVdc Converters in a HVdc Grid." Cigre Working Group B4.57-604, Tech. Rep., 2014.
- [9] Zhong, Q. C., & Weiss, G. (2011). Synchronverters: Inverters that mimic synchronous generators. IEEE Transactions on Industrial Electronics, 58(4), 1259–1267.
- [10] Alipoor, J., Miura, Y., & Ise, T. (2015). Power System Stabilization Using Virtual Synchronous Generator with Alternating Moment of Inertia. IEEE Journal of Emerging and Selected Topics in Power Electronics, 03(2), 451–458.
- [11] Lasseter, R. H., Chen, Z., & Pattabiraman, D. (2020). "Grid-Forming Inverters: A Critical Asset for the Power Grid." IEEE Journal of Emerging and Selected Topics in Power Electronics, 8(2), 925–935.
- [12] Du, W., Chen, Z., Member, S., Schneider, K. P., Member, S., Lasseter, R. H., Fellow, L., Nandanoori, S. P., Tuffner, F. K., & Kundu, S. (2020). "A Comparative Study of Two Widely Used Grid-Forming Droop Controls on Microgrid Small-Signal Stability." IEEE Journal of Emerging and Selected Topics in Power Electronics 8(2), 963–975.
- [13] Liu, J., Miura, Y., & Ise, T. (2016). Comparison of Dynamic Characteristics between Virtual Synchronous Generator and Droop Control in Inverter-Based Distributed Generators. IEEE Transactions on Power Electronics, 31(5), 3600–3611.
- [14] D'Arco, S., & Suul, J. A. (2014). Equivalence of virtual synchronous machines and frequency-droops for converter-based Microgrids. IEEE Transactions on Smart Grid, 5(1), 394–395.
- [15] Collados-Rodriguez, C., Cheah-Mane, M., Cifuentes-Garcia, F., Prieto-Araujo, E., Gomis-Bellmunt, O., Coronado, L., Longas, C., Sanz, S., Martin, M., & Cordon, A. (2022). "Integration of an MMC-HVdc Link to the Existing LCC-HVdc Link in Balearic Islands Based on Grid-Following and Grid-Forming Operation." IEEE Transactions on Power Delivery, 8977(c), 1–11.
- [16] Dong, S., Chi, Y., & Li, Y. (2016). Active voltage feedback control for hybrid multiterminal HVdc system adopting improved synchronverters. IEEE Transactions on Power Delivery, 31(2), 445–455.
- [17] Huang, L., Xin, H., Yang, H., Wang, Z., & Xie, H. (2018). "Interconnecting Very Weak AC Systems by Multiterminal VSC-HVdc Links with a Unified Virtual Synchronous Control." IEEE Journal of Emerging and Selected Topics in Power Electronics, 6(3), 1041–1053.
- [18] Chen, M., Zhou, D., & Blaabjerg, F. (2020). Modelling, Implementation, and Assessment of Virtual Synchronous Generator in Power Systems. Journal of Modern Power Systems and Clean Energy, 8(3), 399–411.
- [19] Y. Liu, M. Hao, Y. He, C. Zang and P. Zeng, "Review and Applications of Virtual Synchronous Machines Technologies," 2019 IEEE Innovative Smart Grid Technologies - Asia (ISGT Asia), Chengdu, China, 2019.
- [20] Q. Duan and C. Zhao, "Improved VSG Controlled SST in a Low-Voltage AC Distribution Network," 2021 IEEE Sustainable Power and Energy Conference (ISPEC), Nanjing, China, 2021, pp. 428-435.
- [21] Qoria, T., Gruson, F., Colas, F., Denis, G., Prevost, T., & Guillaud, X. (2020). Critical Clearing Time Determination and Enhancement of Grid-Forming Converters Embedding Virtual Impedance as Current Limitation Algorithm. 8(2), 1050–1061.

- [22] Paquette, A. D., & Divan, D. M. (2015). Virtual Impedance Current Limiting for Inverters in Microgrids With Synchronous Generators. *IEEE Transactions on Industry Applications*, 51(2), 1630–1638.
- [23] Me, S. P., Zabihi, S., Blaabjerg, F., & Bahrani, B. (2021). Adaptive Virtual Resistance for Post-fault Oscillation Damping with Grid-forming Control. *IEEE Transactions on Power Electronics*, 8993(c), 1–1.
- [24] "IEEE Standard for Interconnection and Interoperability of Inverter-Based Resources (IBRs) Interconnecting with Associated Transmission Electric Power Systems," in *IEEE Std 2800-2022*, vol., no., pp.1-180, 22 April 2022, doi: 10.1109/IEEESTD.2022.9762253.
- [25] Y. Chen, R. Hesse, D. Turschner et al., "Dynamic properties of the virtual synchronous machine (VISMA)," *Renewable Energy and Power Quality Journal*, vol. 1, no. 9, pp. 755-759, May 2011.
- [26] R. Hesse, D. Turschner, and H.-P. Beck, "Micro grid stabilization using the virtual synchronous machine (VISMA)," *Renewable Energy and Power Quality Journal*, vol. 1, no. 7, pp. 676-681, Apr. 2009.
- [27] B. Fan, T. Liu, F. Zhao, H. Wu and X. Wang, "A Review of Current-Limiting Control of Grid-Forming Inverters Under Symmetrical Disturbances," in *IEEE Open Journal of Power Electronics*, vol. 3, pp. 955-969, 2022.